The American Journal of Pathology, Vol. 171, No. 5, November 2007

DOI: 10.2353/ajpath.2007.061275

Immunopathology and Infectious Disease

CCL21 Expression Pattern of Human Secondary Lymphoid Organ Stroma Is Conserved in Inflammatory Lesions with Lymphoid Neogenesis

Antonio Manzo,*† Serena Bugatti,† Roberto Caporali,† Remko Prevo,‡ David G. Jackson,‡ Mariagrazia Uguccioni,§ Christopher D. Buckley,¶ Carlomaurizio Montecucco,† and Costantino Pitzalis*

From the Rheumatology Unit, Guy's, King's, and St. Thomas' School of Medicine, London, United Kingdom; the Institute for Molecular Medicine,‡ John Radcliffe Hospital, Oxford, United Kingdom; the Department of Rheumatology,¶ Birmingham University, Birmingham, United Kingdom; the Chair and Division of Rheumatology,† University of Pavia, Istituto di Ricovero e Cura a Carattere Scientifico Fondazione, Policlinico San Matteo, Pavia, Italy; and the Institute for Research in Biomedicine,§ Bellinzona, Switzerland*

CCL21 is a homeostatic lymphoid chemokine instrumental in the recruitment and organization of T cells and dendritic cells into lymphoid T areas. In human secondary lymphoid organs (SLOs), CCL21 is produced by cells distributed throughout the T zone, whereas high endothelial venules (HEVs) lack CCL21 mRNA. A critical question remains whether the development of ectopic lymphoid tissue (ELT) in chronic inflammation recapitulates the features of SLOs. Thus, we systematically investigated *in situ* the cellular sources of CCL21 in SLOs and ELTs in several human diseases characterized by lymphoid neogenesis. By *in situ* hybridization and the use of combinatorial cell markers, we show that CCL21-producing vessels in inflamed tissues systematically display typical markers of lymphatic vessels, whereas, as in SLOs, ectopic HEVs do not synthesize detectable levels of CCL21. We also provide first-time evidence that a common pattern of CCL21 expression by CD45-negative myofibroblast-like cells localized in extra-HEV position and organized in a fibroblastic reticular network similarly characterizes human SLOs and organized ELTs. Altogether, our results demonstrate that in humans the pattern of CCL21 production in SLOs is maintained during inflammation and that the phenotypic and functional properties of stromal cells, found in SLO T-cell areas, are reproduced at ectopic sites. ***(Am J Pathol 2007, 171:1549–1562; DOI: 10.2353/ajpath.2007.061275)***

CCL21 is a homeostatic chemokine constitutively produced in secondary lymphoid organs (SLOs) where it is involved in CCR7$^+$ naïve and central memory T-cell homing via high endothelial venules (HEVs). CCL21 is also instrumental in the topographical compartmentalization of T cells with CCR7$^+$ mature antigen-bearing dendritic cells (DCs) in the T-cell area.[1–3] Here, CCL21 directly participates to the immunological synapsis, promoting T-cell co-stimulation *in trans* by means of a chemokine-mediated tethering and priming on DCs.[4] Alongside its constitutive function in SLOs, CCL21 is also sufficient to mediate naïve cell extravasation in nonlymphoid inflamed tissues[5] and to promote the constitution of ectopic lymphoid tissue (ELT) in transgenic mice.[6–8] Accordingly, increased expression of CCL21 is strongly associated to the development of lymphoid-like structures in chronically inflamed human tissues, including the joint synovium in rheumatoid arthritis (RA), salivary glands in Sjögren's syndrome (SS), and the intestinal mucosa in ulcerative colitis (UC) and

Supported by the Guy's and St. Thomas' Charity, the Istituto di Ricovero e Cura a Carattere Scientifico Fondazione Policlinico San Matteo, the Arthritis Research Campaign, the Helmut Horten Foundation, the Swiss National Science Foundation, and the European Commission-6th Framework Programme for Research (Innochem).

A.M. and S.B. contributed equally to this work.

Current address of A.M.: Centre for Experimental Medicine and Rheumatology, John Vane Science Centre, William Harvey Research Institute, St. Bartholomew's and Royal London School of Medicine, London, United Kingdom.

Accepted for publication July 19, 2007.

Address reprint requests to Professor Costantino Pitzalis, M.D., Ph.D., F.R.C.P., Head of Centre, Centre for Experimental Medicine and Rheumatology, 2nd Floor, John Vane Science Centre, William Harvey Research Institute, St. Bartholomew's and Royal London School of Medicine, London E1 2AD UK. E-mail: pitzalis@qmul.ac.uk.

Crohn's disease (CD). For a review, see Aloisi and Pujol-Borrell.[9] Suggesting that CCL21 constitutive function may be ectopically reprogrammed in inflammation, CCL21-expressing cells in ELTs have been shown to compartmentalize with T-cell-rich areas and with mature DCs.[10–13]

Although these observations indicate the existence of a functional partnership between CCL21-producing cells with T cells and DCs in the genesis of adaptive responses, a comprehensive characterization of CCL21-producing cells in human lymphoid tissue has not been performed. It is thus unclear whether and to what extent inflammation influences the pattern of CCL21 expression in ELTs or whether the same cellular sources are responsible for CCL21 production in SLOs and ELTs.[5,13,14]

Although CCL21 is constitutively expressed in murine SLOs by T-zone stromal cells,[15] lymphatic vessels, and HEVs[16] as an expression of a species-specific difference, we and others have recently demonstrated that human SLO HEVs lack CCL21 mRNA.[10,17] Instead, the chemokine is produced by lymphatics and nonendothelial cells (non-ECs) within the T area,[17] and translocation of the protein through HEVs has been surmised to mediate T-cell homing,[17] in keeping with the process of transcytosis previously demonstrated for CCL19.[18] Conversely, as opposed to the extravascular synthesis of CCL21 in human SLOs, in inflamed peripheral tissues it has been suggested that CCL21 may be aberrantly induced in ECs of blood vessels and some HEVs, misdirecting naïve T cells to sites of inflammation and triggering the early events of lymphoid neogenesis.[5] Thus, CCL21 production in inflammation would involve specific endothelial differentiation or activation pathways not shared by SLOs and potential target of selective therapies. However, CCL21 is also constitutively produced by lymphatic vessels in peripheral tissues,[5,16,19] where it mediates mature DC and T-cell entry into afferent lymphatics, allowing their migration to draining lymph nodes (LNs).[20–23] Importantly, CCL21-mediated exit through the lymphatics has been shown to be amplified both in experimental inflammation[24] and in human skin inflammatory diseases.[25] In keeping with this concept, $CCL21^+$ lymphatic vessel neoangiogenesis has been described in association with the development of ectopic lymphoid aggregates in renal rejection,[26] indicating that the constitutive cellular sources of CCL21 in peripheral tissues and SLOs can participate in CCL21 production in human ELTs.

To clarify whether chronic inflammation is associated with the appearance of novel sources of CCL21, or rather the pattern of the chemokine is conserved in secondary and ectopic locations, we performed a comparative expression analysis of CCL21 in human SLOs and in a subset of chronic diseases in which immune cells accumulate and form ELTs, addressing the cellular sources of CCL21 in its constitutive environment and in inflammatory sites. We show that the lymphatic system is the source of endothelial CCL21 in inflamed peripheral tissues and that, as in SLOs, blood vessels or HEVs do not synthesize detectable levels of the chemokine in ELTs. We also show, to our knowledge for the first time, that the extra-endothelial expression of CCL21 by smooth muscle actin-positive (SMA^+) stromal cells is a conserved feature in human SLOs and ELTs.

Materials and Methods

Tissues

Synovial samples for *in situ* hybridization, immunohistochemistry (IHC), and immunofluorescence (IF) were obtained from a total of 27 RA patients fulfilling the American College of Rheumatology 1987 revised criteria[27] undergoing joint replacement, synovectomy, or arthroscopic biopsy. The immunophenotypic analysis of CCL21-expressing cells was extended to other inflammatory lesions including minor salivary glands from SS ($n = 21$ patients), intestinal biopsies from UC ($n = 10$ patients) and CD ($n = 6$ patients), and skin biopsies from psoriasis ($n = 4$ patients) and lichen planus ($n = 3$ patients). Patient data, histopathological grading, and treatment schedules are provided in Table 1. Control materials consisted of various normal human SLOs, including two human tonsils, two human mesenteric lymph nodes (MLNs), two cervical lymph nodes (CLNs), two axillary lymph nodes (ALNs), and one human spleen, obtained from individuals undergoing tonsillectomy, surgical resection for neck, colon, or mammary cancer or surgical resection for abdominal trauma. All LNs were free from cancer metastasis. The constitutive pattern of CCL21 expression was also investigated in noninflamed peripheral tissues, including two normal synovial tissues collected during lower limb amputation, two normal minor salivary glands obtained from individuals with suspected amyloidosis[28] (normal histology assessed by routine examination; Congo red-negative), one normal colon obtained during surgical resection for cancer at a minimum of 5 cm from the tumor (normal histology assessed by routine examination), and one normal skin sample obtained from mastectomy. All tissues were fixed in formalin and embedded in paraffin. Four additional RA synovial samples selected for the presence of lymphoid aggregates and HEVs, two human tonsils, and one MLN were embedded in OCT and snap frozen in liquid nitrogen for comparative staining analysis with paraffin-embedded tissues. All procedures involving patient material were approved by the local ethics committee (code no. 08004598/b).

In Situ *Hybridization*

^{35}S-labeled sense and anti-sense RNA probes were generated by *in vitro* transcription (Roche Molecular Biochemicals, Indianapolis, IN). The human CCL21 probe corresponded to positions 6 to 368 of the CCL21 sequence (accession number AB002409).[29] Hybridization and detection of the hybridized probe were performed as previously described.[10,30]

Table 1. Patients' Characteristics

	RA (n = 27)	SS (n = 21)	UC (n = 10)	CD (n = 6)
Age (years) (mean ± SD)	58.5 ± 16	55.5 ± 13	42.4 ± 11.2	38.3 ± 11.8
Female/male	22/5	21/0	3/7	2/4
Disease duration (years) (mean ± SD)	10.6 ± 7.9	1.8 ± 1.5	5.4 ± 4.2	6.7 ± 4.3
ESR (mm/1 hour) (mean ± SD)	32.9 ± 22.3	16.2 ± 9.3	37 ± 20.5	37.8 ± 24.4
CRP (mg/dl) (mean ± SD)	1.6 ± 2.1	0.4 ± 0.2	2.5 ± 2.9	2.7 ± 3.3
No. of RF^+ (%)	16/27 (59.2)	17/21 (80.9)	ND	ND
No. of anti-SSA/Ro^+ and/or anti-SSB/La^+ (%)	1/27 (3.7)	15/21 (71.4)	ND	ND
Use of corticosteroids (%)	20/27 (74.1)	0/21 (0)	9/10 (90)	4/6 (66.7)
Other immunosuppressants				
Methotrexate (%)	12/27 (44.4)	0/21 (0)	0/10 (0)	0/6 (0)
Hydroxycloroquine (%)	11/27 (40.7)	6/21 (28.6)	0/10 (0)	0/6 (0)
Sulfasalazine or mesalazine (%)	0/27 (0)	0/21 (0)	8/10 (80)	3/6 (50)
Leflunomide (%)	3/27 (11.1)	0/21 (0)	0/10 (0)	0/6 (0)
Azathioprine (%)	0/27 (0)	0/21 (0)	1/10 (10)	0/6 (0)
Anti-TNF-α (%)	1/27 (3.7)	0/21 (0)	0/10 (0)	1/6 (16.7)
Pathological scoring*	NA	2.4 ± 3.5	2.4 ± 1.2	3.2 ± 0.7
No. of samples with lymphoid aggregates (%)	15/27 (55.5)	11/21 (52.4)	5/10 (50)	3/6 (50)
No. of samples with $CD21^+$ FDC networks (%)†	5/27 (18.5)	4/21 (19)	1/10 (10)	1/6 (16.7)

RA, rheumatoid arthritis; SS, Sjögren's syndrome; UC, ulcerative colitis; CD, Crohn's disease; ESR, erythrocyte sedimentation rate; CRP, C-reactive protein; RF, rheumatoid factor; ND, not determined; FDC, follicular dendritic cell. Results are expressed as mean ± SD.

*Histological grading of inflammation in the SS specimens was performed according to the method of Greenspan and colleagues,[56] who defined the focus score (FS) as the number of inflammatory infiltrates of at least 50 cells present in 4 mm^2 of gland surface unit. Results are expressed as mean FS (±SD). Histological grading of inflammation in the UC and CD specimens was performed according to the following 0 to 4 scale: 0, normal mucosa; 1, no active inflammation; 2, mild active inflammation; 3, moderate active inflammation; and 4, severe active inflammation.[5] Results are expressed as mean ± SD. NA, not applicable.

†Data on the prevalence of $CD21^+$ FDC networks have been obtained by a single cutting level analysis.

IHC

IHC on paraffin-embedded tissue sections was performed as previously described in detail.[10,30] The following primary antibodies were used: goat anti-human CCL21 (IgG; R&D Systems, Minneapolis, MN), mouse anti-human CD31 (IgG1, clone 1A10; Novocastra, Newcastle-on-Tyne, UK), mouse anti-human CD34 (IgG1, clone QBEnd/10; Novocastra), rat anti-human/mouse peripheral lymph node addressin (PNAd) (IgM, clone MECA 79; PharMingen, San Diego, CA), mouse anti-human lymphatic vessel endothelial hyaluronan receptor (LYVE-1) (IgG1, clone 8C; provided by D.G. Jackson, Institute for Molecular Medicine, John Radcliffe Hospital, Oxford, UK), goat anti-human LYVE-1 (IgG; R&D Systems), mouse anti-human podoplanin (IgG1, clone 4D5aE5E6; Bender MedSystems, Wien, Austria), rat anti-human D6 (IgG2a, clone 196124; R&D Systems), rabbit anti-human CD3 (IgG; DAKO, Carpinteria, CA), mouse anti-human CD20 (IgG2a, clone L26; DAKO), mouse anti-human CD21 (IgG1, clone 1F8; DAKO), goat anti-human CXCL13 (IgG, R&D Systems), goat anti-human CCL19 (IgG, R&D Systems), mouse anti-human DC-lysosome-associated membrane protein (LAMP) (IgG1, clone 104-G4; Immunotech, Marseilles, France), mouse anti-human CD45 (IgG1, clones 2B11 + PD7/26; DAKO), and mouse anti-human SMA (IgG2a, clone 1A4; DAKO). Negative staining control experiments were performed either by omitting the primary antibody or by using a control isotype-matched antibody. For double-staining experiments, dewaxed and rehydrated sections were heated at 96°C in target retrieval solution (DAKO), washed in Tris-buffered saline (TBS), and incubated with Protein Block Serum Free (DAKO). The first primary antibody was applied, followed by incubation with peroxidase-conjugated rabbit anti-mouse IgG (DAKO). Sections were then developed using 3,3′-diaminobenzidine tetrahydrochloride (Sigma, St. Louis, MO), blocked in distilled water, washed in TBS, and again incubated in Protein Block Serum Free. The second primary antibody was applied, followed by incubation with biotinylated donkey anti-goat IgG (Jackson ImmunoResearch Laboratories, Cambridgeshire, UK) and amplification with streptavidin biotin complex-alkaline phosphatase (DAKO). Sections were developed using New Fuchsin substrate kit (DAKO), counterstained with Meyer's hematoxylin (Merck, Rahway, NJ) and mounted with Aquamount mounting medium (BDH, Poole, UK). Primary and secondary antibodies were diluted in DAKO antibody diluent.

IF

Double-color IF for CCL21 and PNAd was performed on OCT-embedded frozen samples of four RA synovial membranes, two human tonsils, and one human MLN. Six-μm-thick sections were cut, allowed to dry on glass slides, and fixed for 15 minutes in acetone. Sections were then washed in TBS and incubated with Protein Block Serum Free. Rat anti-human/mouse PNAd was applied, followed by incubation with donkey anti-rat IgG fluorescein isothiocyanate-conjugated (Jackson ImmunoResearch Laboratories). After TBS washing and an additional blocking in 10% human serum diluted in TBS, goat anti-human CCL21 was applied, followed by incubations with donkey anti-goat IgG biotinylated (Jackson ImmunoResearch Laboratories) and rhodamine Red-X-conjugated streptavidin (Jackson ImmunoResearch Laboratories). Sections were counterstained using DAPI (4,6-diamidino-2-phenylindole) (Sigma) and

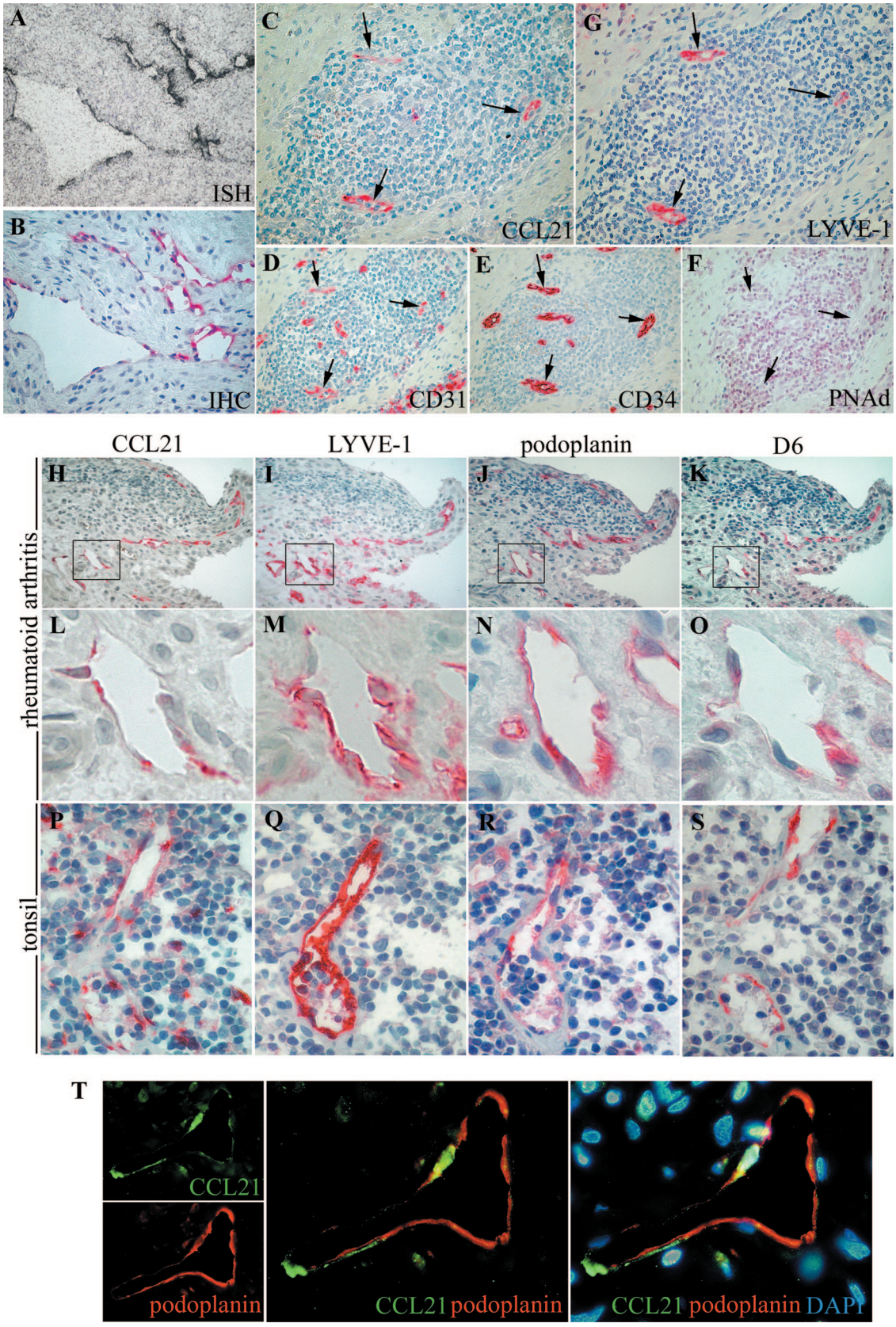
A
ISH
B
IHC
C
CCL21
G
LYVE-1
D
CD31
E
CD34
F
PNAd
CCL21
LYVE-1
podoplanin
D6
rheumatoid arthritis
tonsil
H
I
J
K
L
M
N
O
P
Q
R
S
T
CCL21
podoplanin
CCL21 podoplanin
CCL21 podoplanin DAPI

mounted with fluorescence mounting medium (DAKO). Negative staining control experiments were performed by using a control isotype-matched antibody.

Double-color IF for CCL21 or CCL19 and CD45 or SMA on paraffin-embedded sections were performed analogously to IHC experiments. The following secondary antibodies were used: donkey anti-rat IgG fluorescein isothiocyanate for CD45 and SMA and donkey anti-goat IgG biotinylated followed by amplification with Red-X-conjugated streptavidin for CCL21 and CCL19 (all from Jackson ImmunoResearch Laboratories). All IF procedures were performed in darkness. Sections were examined by IF microscopy (BX51; Olympus, Hamburg, Germany) and confocal microscopy (Leica TCS SP2; Leica Microsystems GmbH, Wetzlar, Germany).

Histological Data Evaluation and Quantification

The immunocharacterization of CCL21-producing vessels in RA synovium was performed on 3-μm-thick consecutive sections stained for pan-vascular markers (CD31 and CD34),[31,32] HEV markers (PNAd),[33] and a subset of markers that have been shown to be specific for the lymphatic endothelium, including LYVE-1, podoplanin, and D6.[34–36] Because of the heterogeneous distribution of CCL21$^+$ vessels, quantification and immunophenotypic analysis were performed in CCL21 vascular hot spots or areas containing the highest density of CCL21$^+$ vessels, according to a method first used for the estimation of new blood vessel formation in breast tumor.[37] Three hot spots per section were selected. In each spot, positive vessels were counted in 10 consecutive fields at high magnification (×400). The median number of counted CCL21$^+$ vessels/sample in the nine samples with the presence of vascular CCL21 (see Results) was 50, with a range of 30 to 202. Of counted CCL21$^+$ vessels 99.2% were recognized by two independent observers on serial sections stained for vascular markers. To confirm the co-localization between CCL21 and lymphatic markers on ECs, in six samples double IF stainings for CCL21 and podoplanin were performed, and vessels were examined inside and outside of hot spots.

The immunocharacterization of nonendothelial CCL21-expressing cells as well as CCL19$^+$ cells in human SLOs was assessed for each tissue in 10 consecutive high-power fields (×1000) (median number of counted CCL21$^+$ cells/sample, 178; range, 86 to 242; median number of counted CCL19$^+$ cells/sample, 83; range, 72 to 102). In RA synovium, attributable to heterogeneous distribution of CCL21$^+$ and CCL19$^+$ cells, the analysis was performed according to the hot spot method (median number of counted CCL21$^+$ cells/sample, 43; range, 7 to 100; median number of counted CCL19$^+$ cells/sample, 34; range, 4 to 82).

The prevalence of CCL21$^+$SMA$^+$ cells in the synovial lymphoid tissue was evaluated in the 15 samples with lymphoid aggregates (see Results and Table 1) and expressed as the percentage of aggregates of large dimensions (radial cell count from the more centrally located vessel to the identifiable edge of the aggregate >10 cells[10]) positive for CCL21 and SMA. The total number of large-size aggregates counted was 269, with a median number/sample of 12 (range, 3 to 44).

LN Primary Cell Separation and Cell Lines

Primary cells from one normal human MLN were obtained by enzymatic digestion with 0.2% collagenase in high-glucose Dulbecco's modified Eagle's medium (GIBCO, Invitrogen, Carlsbad, CA) containing 10% fetal bovine serum (GIBCO, Invitrogen) and 100 U/ml penicillin plus 100 μg/ml streptomycin sulfate (GIBCO, Invitrogen). After 4 hours of incubation at 37°C, cells were collected, washed, and used for cytospin preparations and RNA extraction. RA synovium, spleen, and LN fibroblast cell lines were kindly provided by Debbie Hardie (Department of Rheumatology, Birmingham University, Birmingham, UK).

IF on Cytospins

Double-color IF for CCL21 and SMA on freshly isolated cells and cell lines was performed analogously to IF experiments on frozen tissue samples. Cells were fixed with 2.5% paraformaldehyde for 20 minutes at room temperature and permeabilized with TBS and 0.3% saponin.

RNA Extraction and Quantitative Real-Time PCR

Total RNA was extracted from isolated cells using the RNeasy mini kit (Qiagen, Hilden, Germany) following the manufacturer's instructions and was reverse-transcribed into cDNA with the ThermoScript reverse transcriptase-PCR system (Invitrogen). Quantitative real-time PCR was performed using Hot Start DNA polymerase (Qiagen) in

Figure 1. CCL21-producing endothelial structures in rheumatoid synovitis display lymphatic features. *In situ* hybridization (**A**) and IHC (**B**) for CCL21 in parallel tissue sections of rheumatoid synovial membrane demonstrate co-localization between CCL21 mRNA (**A**, in black) and protein (**B**, in red) in a subset of vascular structures. **C–G:** A synovial lymphoid aggregate is shown on serial tissue sections immunostained for CCL21 (**C**, in red), CD31 (**D**, in red), CD34 (**E**, in red), PNAd (**F**, in red), and LYVE-1 (**G**, in red). **Arrows** indicate the same vascular structures analyzed in parallel sections. Note that all CCL21-positive vessels (**black arrows**) are LYVE-1-positive lymphatic vessels. **H–K:** IHC on sequential sections of a synovial hypertrophic villous showing a subset of vascular structures immunostained for CCL21 (**H**, in red), LYVE-1 (**I**, in red), podoplanin (**J**, in red), and D6 (**K**, in red). All CCL21-positive vessels (**H**) are LYVE-1-positive (**I**) podoplanin-positive (**J**), and D6-positive (**K**). The synovial vessel delimited by the **black square** in **H–K** is shown at high magnification in **L–O**, demonstrating the co-localization of CCL21 (**L**), LYVE-1 (**M**), podoplanin (**N**), and D6 (**O**). **P–S:** High-magnification views of serial sections of tonsil showing endothelial co-localization of CCL21 (**P**, in red) with LYVE-1 (**Q**, in red), podoplanin (**R**, in red), and D6 (**S**, in red). **T:** Single color separations and color merges of double IF staining for CCL21 (in green) and podoplanin (in red) on rheumatoid synovium, showing the co-localization of the two markers. Counterstaining with DAPI in blue. Original magnifications: ×400 (**A–G**); ×200 (**H–K**); ×1000 (**L–T**).

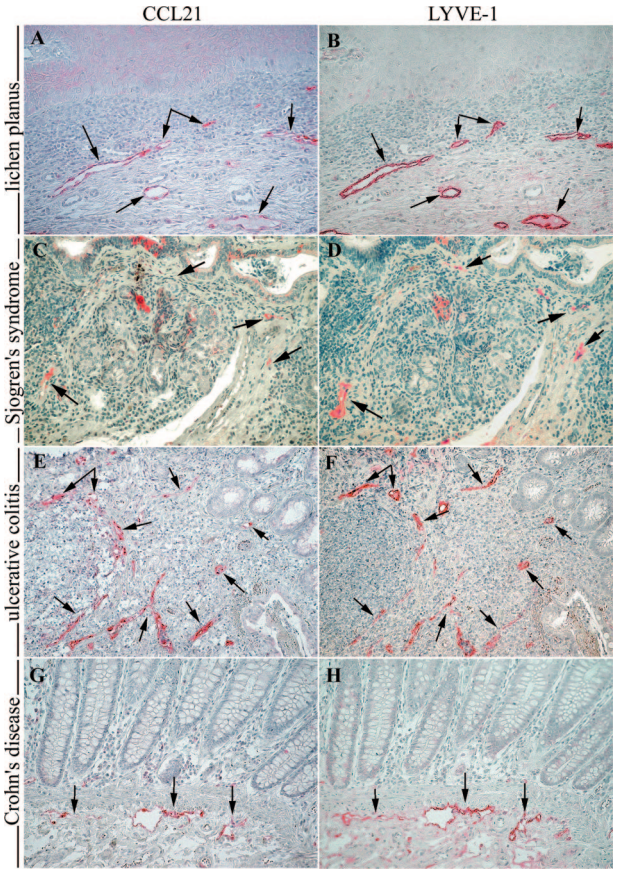

Figure 2. The lymphatic nature of CCL21$^+$ endothelial structures is a shared feature of different human chronic inflammatory diseases. Serial immunostaining for CCL21 (**A**, **C**, **E**, and **G**; in red) and LYVE-1 (**B**, **D**, **F**, and **H**; in red) is shown on sections of lichen planus (**A** and **B**), SS (**C** and **D**), UC (**E** and **F**), and CD (**G** and **H**). All CCL21-positive vessels are LYVE-1-positive. **Black arrows** indicate the same vascular structures analyzed in parallel sections. Note that CCL21-expressing vessels are LYVE-1-positive both in tissue areas characterized by dense immune-cell infiltration with lymphoid aggregates (**E** and **F**) and in noninfiltrated areas (**G** and **H**). Original magnifications, ×200.

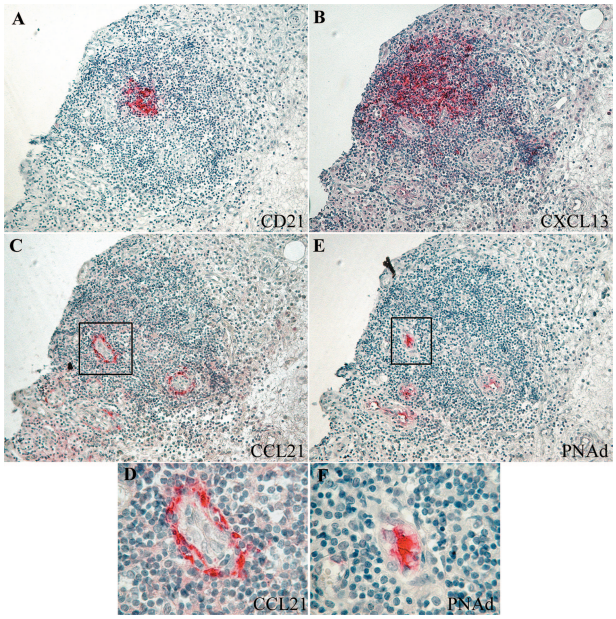

Figure 3. Distribution of periendothelial CCL21$^+$ cells in HEVs of ectopic GC-like structures. Serial immunostaining for CD21 (**A**), CXCL13 (**B**), CCL21 (**C**), and PNAd (**D**) is shown on tissue sections of rheumatoid synovium, illustrating the presence of CCL21-expressing cells localized perivascularly (**C**) in close association to PNAd-positive HEVs (**E**) within a highly organized aggregate characterized by a CD21$^+$ follicular DC network (**A**) and CXCL13 expression (**D**). In **E** and **F**, a detail of the vessel delimitated by the **black square** in **C** and **E** is shown at high magnification, revealing the presence of CCL21-expressing non-ECs (**D**) adherent to the abluminal side of the PNAd-positive HEV endothelium (**F**). Original magnifications: ×200 (**A–D**); ×1000 (**D** and **F**).

the presence of 0.1× SYBR Green (Molecular Probes, Invitrogen) using an Applied Biosystem 7900HT sequence detector (Applied Biosystems, Foster City, CA). A serial dilution of a cDNA from human LN was used for a standard curve. Gene expression was calculated using a standard curve and normalized for the expression of the housekeeping gene β-actin. Primers used were *CCL21:* forward 5′-CAAGCTTAGGCTGCTCCATC-3′, reverse 5′-TCAGTCCTCTTGCAGCCTTT-3′; and *β-actin:* forward 5′-CACGGCTGCTTCCAGCTC-3′, reverse 5′-CACAGGACTCCATGCCCAG-3′.

Results

CCL21-Producing Endothelial Structures in Rheumatoid Synovitis Display Lymphatic Features

In keeping with previous reports,[5,10,11] we observed high expression of CCL21 in ECs of vascular structures in a proportion of RA synovial tissues. Single cutting level analysis on paraffin sections showed the presence of CCL21$^+$ vessels in 9 of 27 samples, whereas the absence or only the occasional presence of these structures was observed in the other specimens included in the study. Parallel *in situ* hybridization and IHC experiments on 3-μm-thick consecutive sections demonstrated CCL21 mRNA and protein co-localization in all vessels analyzed (Figure 1, A and B).

The immunophenotypic analysis of CCL21-producing vessels revealed that all were CD31$^+$, confirming their vascular nature (Figure 1, C and D). CD34 staining was instead variable, with some CCL21$^+$ vessels displaying high levels of CD34 (Figure 1, C and E) and some others being CD34-low/negative (not shown). No PNAd expression was found in ECs of CCL21$^+$ vascular structures (Figure 1, C and F). Notably, LYVE-1 (a marker of the lymphatic endothelium) stained 100% of CCL21-producing vessels (Figure 1, C and G) and, vice versa, CCL21 expression was recognized in 97.6 ± 1.2% (mean ± SD) of LYVE-1$^+$ vessels. Conversely, CD31$^+$CD34$^+$LYVE-1-negative vessel did not reveal definite CCL21 expression in the cytoplasm of ECs, showing only occasionally a weak and poorly defined CCL21 signal. To confirm the identity of CCL21$^+$LYVE-1$^+$ vessels as lymphatics, we stained consecutive sections with antibodies against podoplanin and D6. These experiments clearly demonstrated that all CCL21$^+$LYVE-1$^+$ vessels also displayed podoplanin immunoreactivity (Figure 1, H–J and L–N) and that some of them were also positive for D6, although all D6$^+$ vessels were CCL21$^+$LYVE-1$^+$podoplanin$^+$ (Fig-

ure 1, H–K and L–O). Results were confirmed by double IF staining for CCL21 and podoplanin, showing podoplanin staining in 100% of CCL21$^+$ vessels independently of their size and their location within the synovial tissue (Figure 1T).

To exclude that synovial blood vessel ECs aberrantly expressed CCL21 only in tissues with organized lymphoid aggregates, we analyzed our samples for the presence of specific lymphoid tissue-like features (T-B cell compartmentalization and CD21$^+$ follicular DC networks). These experiments confirmed that CCL21$^+$ vessels both in synovial tissues with diffuse infiltration (n = 12/27, 44.4%) and in those with lymphoid aggregates, with (n = 5/27, 18.5%) or without (n = 10/27, 37.1%) detectable germinal centers (GCs), were 100% positive for LYVE-1 and podoplanin. Similarly, in tonsil paraffin sections, CCL21 was found in the cytoplasm of LYVE-1$^+$podoplanin$^+$ ECs displaying variable D6 expression (Figure 1, P–S).

The Lymphatic Nature of CCL21$^+$ Endothelial Structures Is a Shared Feature of Different Human Chronic Inflammatory Diseases

To test whether the findings obtained in RA synovitis are applicable to other human chronic inflammatory conditions, we extended the immunocharacterization of CCL21$^+$ vessels to other inflamed tissues. All CCL21$^+$ endothelial structures were LYVE-1$^+$ both in psoriasis (not shown) and in lichen planus (Figure 2, A and B), two autoimmune skin inflammatory diseases in which lymphoid neogenesis does not commonly occur. The same findings were observed in SS (Figure 2, C and D), UC (Figure 2, E and F), and CD (Figure 2, G and H), where a lymphoid neogenetic organization can be prominent (Table 1). Again, CCL21$^+$ endothelial structures were 100% LYVE-1$^+$ irrespectively to their localization and association with the ELT. The observed CCL21 expression by the lymphatic

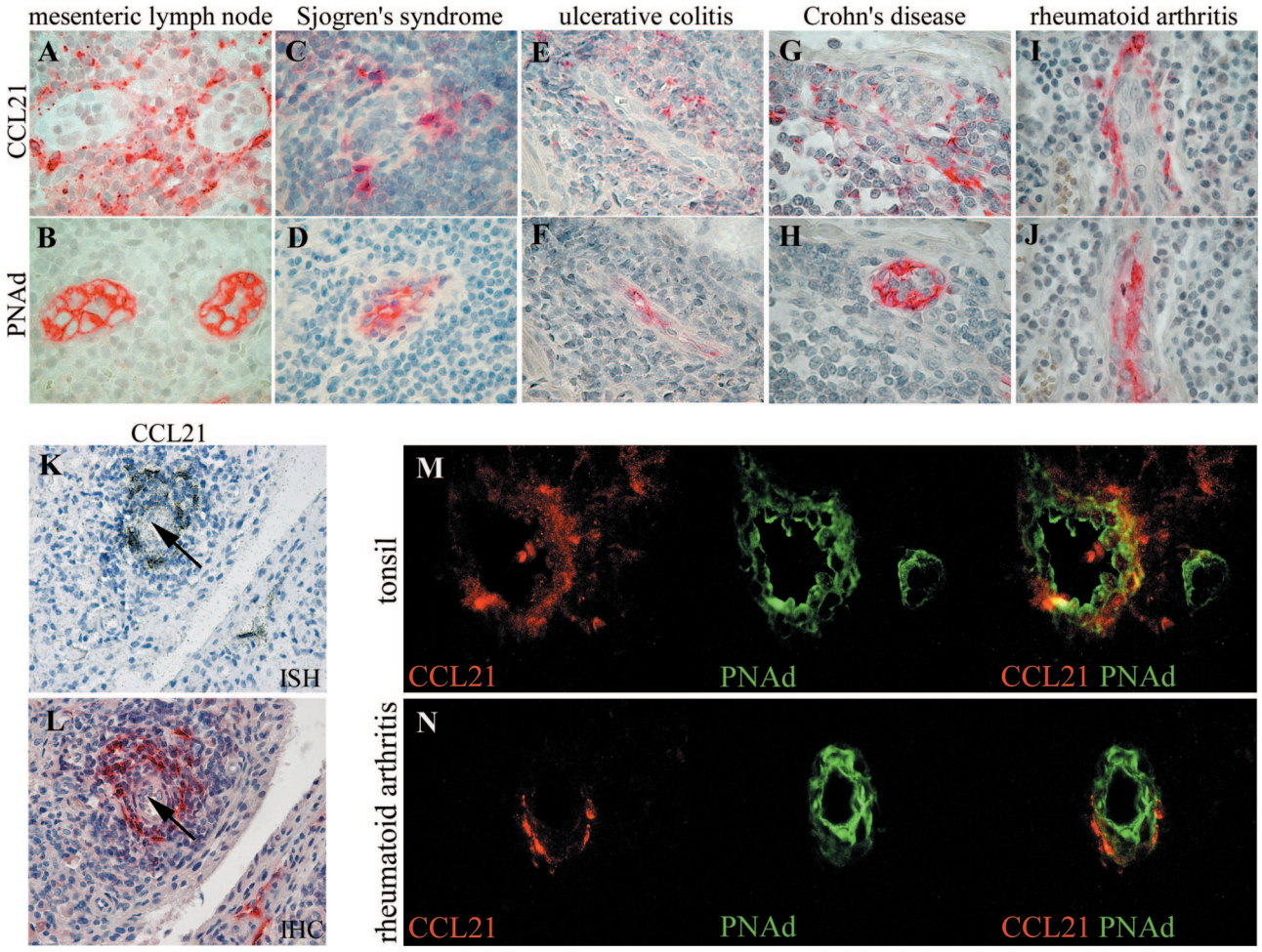

Figure 4. Preserved relationship between CCL21 production and HEVs in human SLOs and ELTs. **A–J:** Immunostaining for CCL21 (**A**, **C**, **E**, **G**, and **I**; in red) and parallel immunostaining for PNAd (**B**, **D**, **F**, **H**, and **J**; in red) on paraffin-embedded tissues of human MLN (**A** and **B**), SS salivary gland (**C** and **D**), UC intestinal wall (**E** and **F**), CD intestinal wall (**G** and **H**), and RA synovium (**I** and **J**) reveal the presence of CCL21-expressing non-ECs adherent to the abluminal side of PNAd-positive HEVs both in human SLOs and within ectopic lymphoid aggregates in lymphoid neogenetic diseases. **K** and **L:** IHC (**K**) and *in situ* hybridization (**L**) for CCL21 in consecutive synovial tissue sections of RA confirm the complete co-localization between CCL21 protein expression (**K**, in red) and mRNA production (**L**, in black) within non-ECs surrounding a vessel with HEV morphology. **Black arrows** indicate blood vessel ECs lacking detectable levels of CCL21, despite the presence of adjacent CCL21-positive cells. **M** and **N:** Single color separations and color merges of double IF staining for CCL21 (in red) and PNAd (in green) on cryosections of human tonsil (**M**) and rheumatoid synovial tissue (**N**). The strongest CCL21 immunostaining is seen within PNAd-positive HEVs at their basal side, whereas PNAd staining is strongest at the luminal face. Original magnifications: ×1000 (**A–J**, **M**, and **N**); ×400 (**K** and **L**).

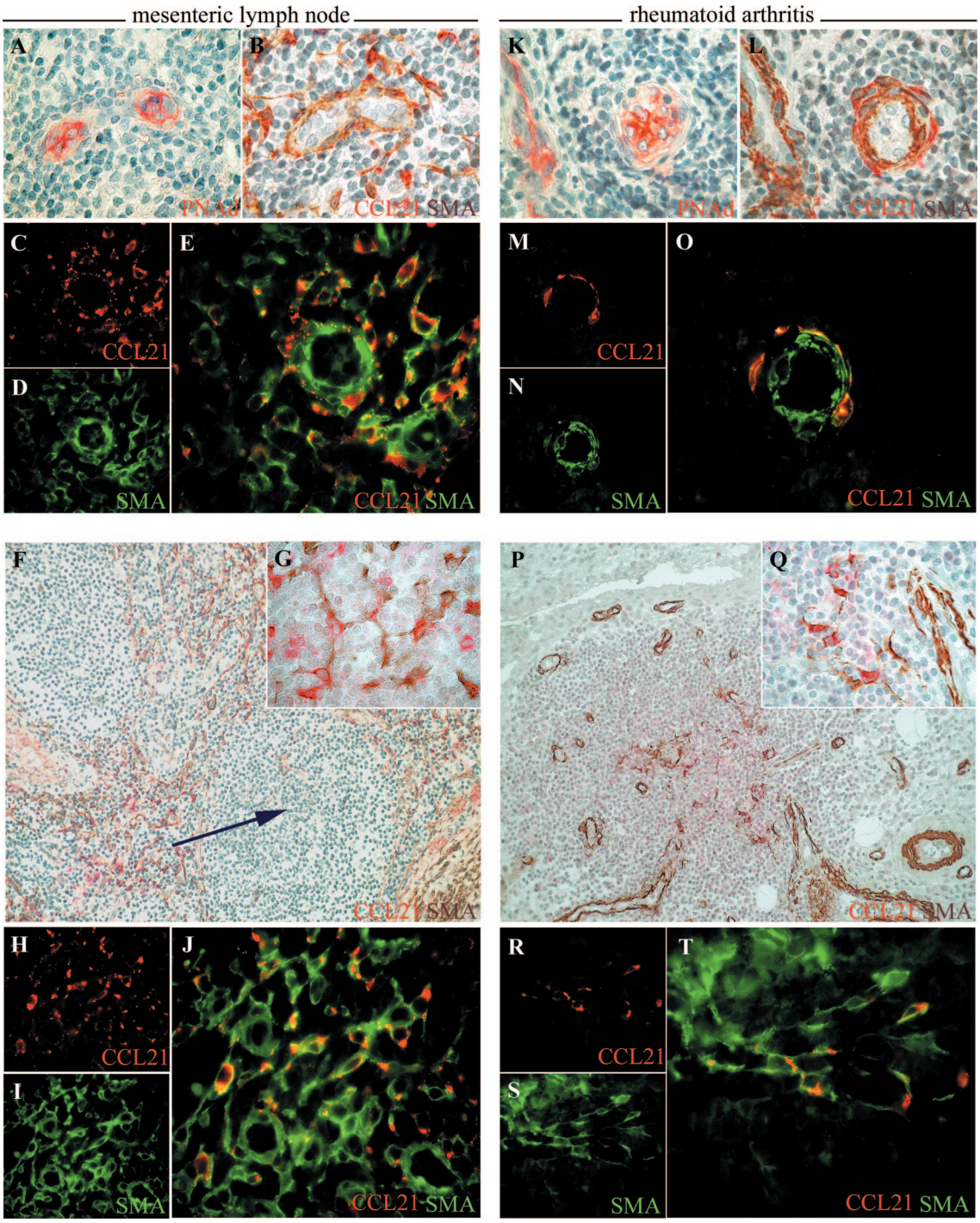

Figure 5. SMA-positive stromal cells express CCL21 in human MLNs and in synovial ELT. **Left:** Stainings on paraffin-embedded sections of human MLN are shown. **A** and **B:** IHC for PNAd (**A**, in red) and double IHC for SMA (**B**, in brown) and CCL21 (**B**, in red) on serial tissue sections showing CCL21-positive cells in periendothelial localization around a PNAd-positive HEV and displaying SMA immunoreactivity. **C–E:** Single color separations (**C** and **D**) and double merge (**E**) of double IF for CCL21 (**C** and **E**; in red) and SMA (**D** and **E**; in green) show the co-localization between the two antibodies (revealed by yellow signal in **E**) in association to a vessel with HEV morphology. **F:** Double IHC for CCL21 (in red) and SMA (in brown) is shown on a tissue area at low magnification, demonstrating the co-localization between CCL21 and a network of SMA-positive cells distributed throughout the T area and connecting vascular structures. Note the absence of the SMA-positive reticulum inside a germinal center (**black arrow**). In **G**, a detail of the area represented in **F** is shown at high magnification. **H–J:** Single color separations (**H** and **I**) and color merge (**J**) of double IF for CCL21 (**H** and **J**; in red) and SMA (**I** and **J**; in green) show the co-localization between CCL21-expressing cells within the T-cell area and SMA-positive reticular cells, as revealed by yellow signal in **J**. **Right:** Stainings on paraffin-embedded sections of rheumatoid synovial membrane are shown. **K** and **L:** single IHC for PNAd (**K**, in red) and double IHC for SMA (**L**, in brown) and CCL21 (**L**, in red) on serial sections show that CCL21-positive cells adherent to a PNAd-positive HEV are SMA-positive. **M–O:** Single color separations (**M** and **N**) and color merge (**O**) of double IF for CCL21 (**M** and **O**; in red) and SMA (**N** and **O**; in green) confirms the co-localization of the two markers (yellow signal in **O**) in association to a synovial vessel with HEV morphology. **P:** Double IHC for CCL21 (in red) and SMA (in brown) is shown at low magnification on a synovial hypertrophic villous, demonstrating the co-localization between CCL21 and a network of SMA-positive cells connecting vascular structures within a lymphoid aggregate. In **Q**, high magnification of a detail of picture **P** is shown. **R–T:** Single color separations (**R** and **S**) and color merge (**T**) of double IF for CCL21 (**R** and **T**; in red) and SMA (**S** and **T**; in green) confirms the co-localization of the two markers (yellow signal in **T**) within reticular cells unrelated to vascular structures. Experiments analyzed under IF microscopy. Original magnifications: ×1000 (**A–E**, **G–O**, and **Q–T**); ×200 (**F** and **P**).

endothelium was consistent with results obtained in non-inflamed peripheral tissues (normal synovium, colon, and skin), where CCL21$^+$ vessels revealed intense staining for LYVE-1 (not shown). The above results demonstrate that inflammation and ectopic lymphoid neogenesis can take place in the absence of aberrant induction of CCL21 in blood vessels and that lymphatics can be the exclusive endothelial source of CCL21 in ELTs as well as in SLO.[17]

The Peri-HEV Synthesis of CCL21 Is Reprogrammed in ELTs

Although CCL21 production was not detected in HEV ECs, in some lymphoid aggregates in SS, UC, CD, and RA, CCL21-expressing cells were recognized in an extravascular location, sometimes tightly adherent to the basal side of a proportion of PNAd$^+$ HEV. This pattern was also identified inside highly organized lymphoid clusters as inferred by the presence of follicular DC networks and CXCL13 expression (Figure 3). Parallel *in situ* hybridization experiments confirmed the lack of detectable levels of CCL21 mRNA in ectopic HEV endothelium, even when surrounded by high numbers of CCL21-producing cells, which demonstrated stringent matching between CCL21 mRNA and protein expression (Figure 4). Periendothelial CCL21 was highly restricted to lymphoid aggregates in all tissues and diseases analyzed and was reminiscent of the distribution of CCL21-expressing cells observed in human tonsils and LNs on paraffin sections. Figure 4, A–J, illustrates the consistency of CCL21 peri-HEV expression between human SLOs and the ELT in SS, UC, CD, and RA. Figure 4, K and L, shows the co-localization of CCL21 protein and mRNA in ELTs. As a proof of the strong association between this pattern with inflammation and lymphoid tissue organization (both ectopic and orthotopic), we could not observe any perivascular expression of CCL21 in psoriasis, lichen planus, and noninflamed control tissues including normal synovium, minor salivary glands, colon, and skin (not shown).

To allow a comparison with formalin-fixed tissues, we performed double IF stainings for CCL21 and PNAd on cryosections. These experiments showed CCL21 protein within and at the basal side of HEVs in human SLOs (Figure 4M), in accordance to the recent findings from Carlsen and colleagues.[17] The same pattern was confirmed in some HEVs of RA lymphoid neogenetic lesions (Figure 4N). Taken together, these results demonstrate that the anatomical relationship between CCL21 and the vascular system is qualitatively preserved in SLOs and ELTs, suggesting the existence of a conserved cellular program regulating CCL21 expression in human lymphoid tissues.

SMA$^+$ Stromal Cells Express CCL21 in Peri-HEV Location and in T-Cell-Rich Areas Both in ELTs and Human SLOs

To characterize the nature of extra-endothelial CCL21-expressing cells in human SLOs and ELTs, we performed double IHC and IF staining on paraffin-embedded samples. To provide direct evidence of the hematopoietic or stromal nature of CCL21-producing cells, we first examined CCL21 and CD45 staining. These experiments demonstrated that, in human LNs and tonsils, all CCL21$^+$ cells in close proximity to vascular structures with HEV morphology were CD45-negative. CD45-negative, CCL21$^+$ stromal cells were also found scattered within the T-cell areas and unrelated to HEVs. Interestingly, identical results were obtained in RA synovium ELTs, where CCL21$^+$ cells inside the aggregates were mostly CD45-negative,

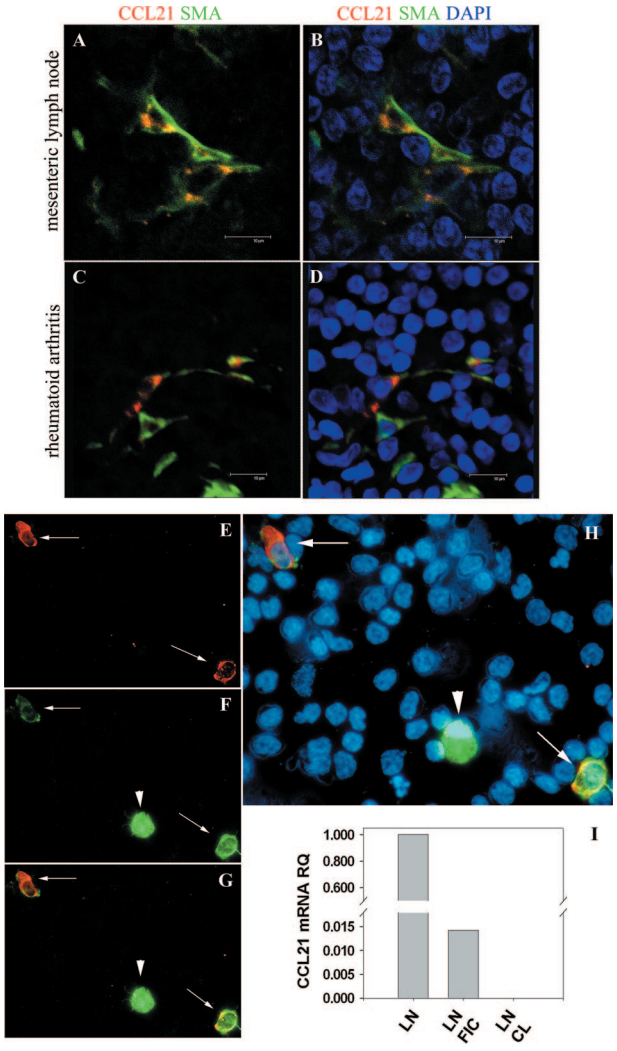

Figure 6. Intracytoplasmic localization of CCL21 in SMA-positive cells. **A–D:** Double IF for CCL21 (in red) and SMA (in green) is shown in human MLN (**A** and **B**) and rheumatoid synovial membrane (**C** and **D**) analyzed by confocal microscopy. **B** and **D** show the images represented in **A** and **B** with DAPI counterstaining to highlight the cell nucleus (in blue). CCL21 signal is detected within SMA-positive reticular cells both in human SLOs and in the ELT of rheumatoid synovitis. **E–H:** Single color separations (**E** and **F**) and color merges (**G** and **H**) of double IF staining for CCL21 (**E**, **G**, **H**, in red) and SMA (**F**–**H**, in green) on a cytospin preparation obtained from freshly isolated LN cells, demonstrating co-localization of CCL21 and SMA *ex vivo* in two cells indicated by **white arrows** (yellow signal in **G** and **H**). In **H**, cell nuclei are counterstained in blue with DAPI. **Arrowheads** indicate a SMA-positive cell lacking CCL21 staining. **I:** CCL21 gene expression levels in intact LN, in the freshly isolated lymph node cells analyzed in **E–H** (LN FIC), and in a lymph node fibroblast cell line (LN CL) determined by quantitative PCR. RQ, relative quantification. Data are normalized for β-actin. Original magnifications, ×1000.

both in peri-HEV location and scattered within lymphoid clusters (not shown).

Morphologically, most of CD45-negative CCL21^{+} cells both in human SLOs and in ELTs were characterized by a spindle-shaped or irregular cell body with branching processes. This pattern is strongly reminiscent to that of fibroblastic reticular cells (FRCs), pericytes, and myofibroblasts, different subsets of mesenchymal cells capable to *trans*-differentiate one into another[38,39] and sharing the expression of SMA.[40–42]

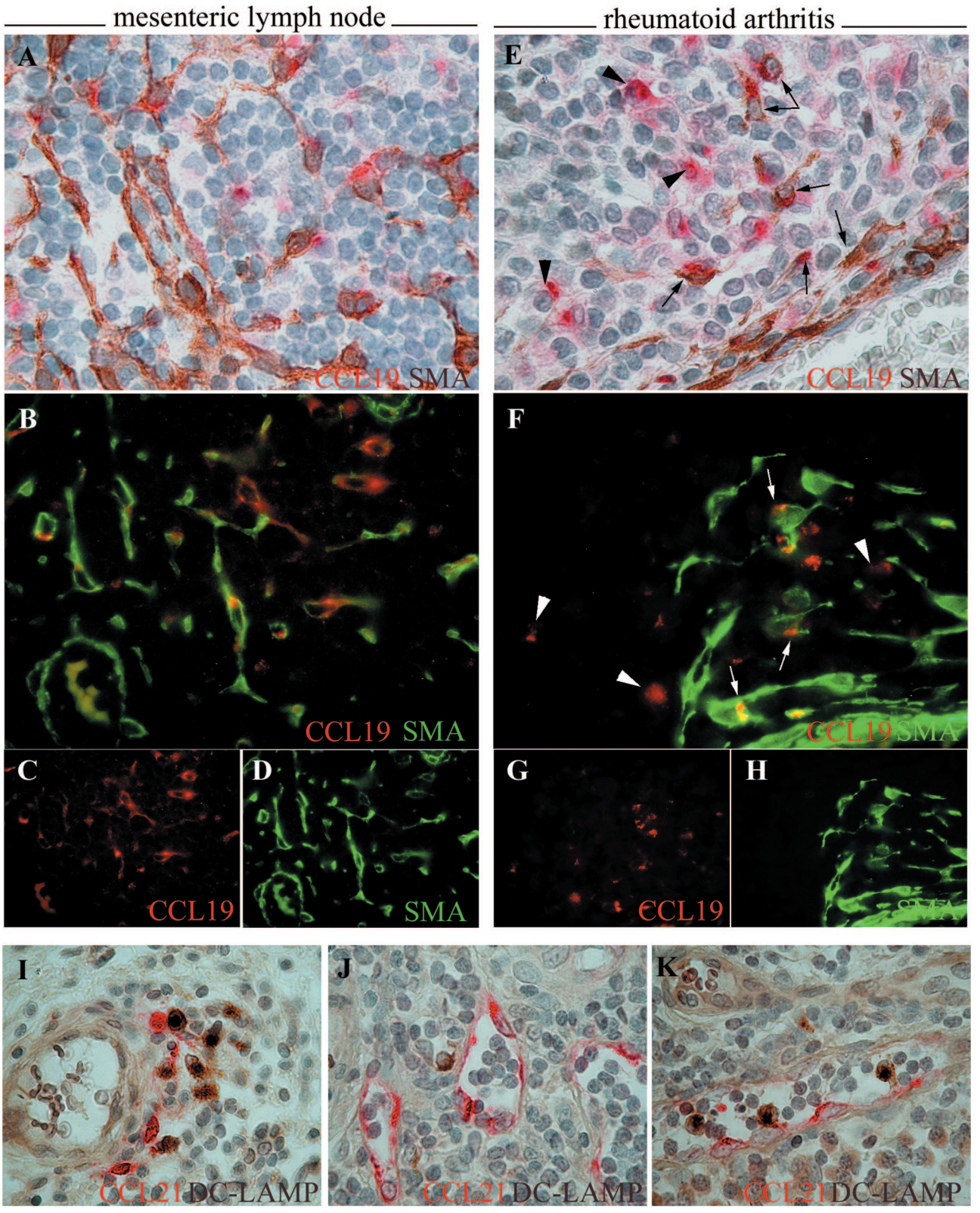

We thus performed double IHC and IF experiments for CCL21 and SMA in SLOs and ELTs. In human LNs from various anatomical districts (mesenteric, cervical, axillary), we observed stringent co-localization of periendothelial CCL21 and SMA in all areas examined (Figure 5, A–E). Furthermore, $CCL21^+$ cells scattered within the T-cell area co-localized with a meshwork of SMA^+ dendritiform cells extending from the subcapsular sinus and disseminated throughout the node, where they created a connection among HEVs (Figure 5, F–J). Altogether, CCL21-expressing cells were 92.7 ± 3.4% (mean ± SD) SMA^+ in MLNs, 88.2 ± 1.2% in CLNs, and 84.2 ± 1% in ALNs. Similar co-localization was demonstrated in spleen (89.5%) and in tonsils, although in the latter the SMA^+ meshwork appeared less developed and $CCL21^+$ cells lacked SMA staining in certain tissue areas (29.3 ± 15%). No co-localization was observed between T-cell area SMA^+ cells and LYVE-1 in all SLOs analyzed (not shown).

Results in RA ELT were consistent with those obtained in human LNs. Indeed, peri-HEV CCL21-expressing cells were all SMA^+ (Figure 5, K–O), and SMA immunoreactivity was also demonstrated in LYVE-1-negative, $CCL21^+$ cells scattered within lymphoid aggregates. Altogether, 94.7 ± 6% of CCL21-expressing cells exhibited SMA staining. $CCL21^+SMA^+$ cells were recognized in 150 of 269 (55.8%) large aggregates (median percentage of positive aggregates/sample, 66.7%; range, 12.5 to 100%), their presence not being strictly related to GC^+ follicles. Although most of these cells were either isolated or organized in small clusters (Figure 5H), the constitution of a more developed LN-like $CCL21^+SMA^+$ meshwork connecting vascular structures could be demonstrated in a proportion of large-size aggregates (Figure 5, P–T). The analysis of lymphoid neogenetic lesions in SS, UC, and CD revealed the presence of SMA^+ CCL21-expressing cells also in these pathological settings. In normal control tissues, instead, no periendothelial or scattered expression of CCL21 was found despite the presence of SMA^+ cells in perivascular location (not shown).

Confocal microscopy examinations confirmed CCL21 localization in the cytoplasm of SMA^+ cells both in SLOs and RA ELTs (Figure 6, A–D). CCL21 staining was also observed in freshly isolated SMA^+ cells obtained after LN enzymatic digestion and analyzed at the single-cell level on cytospin preparations (Figure 6, E–H). Parallel experiments by quantitative PCR on the same cells confirmed local expression of CCL21 mRNA (Figure 6I). Conversely, despite the presence of SMA^+ cells between passages 6 and 10, no significant CCL21 expression was recognized in LN, spleen, and RA synovium fibroblastic lines either in basal conditions or on stimulation with tumor necrosis factor-α and lymphotoxin $\alpha 1\beta 2$ throughout 72 hours.

SMA^+ Cells in Human SLOs and ELTs Express CCL19 and Co-Localize with Mature DCs

To compare additional features of SMA^+ cells in SLOs and ELTs, we investigated the expression of CCL19, the other known ligand for CCR7, which has been previously reported in FRCs in murine SLOs.[15] Interestingly, double IHC and IF experiments revealed the capacity of SMA^+ cells both in SLOs and in RA synovium ELT to express CCL19 (Figure 7, A–H), providing further evidence that the constitutive cellular properties of SLO stroma are reprogrammed in inflammatory ELT. Altogether, 91.7 ± 5.2% (mean ± SD) of $CCL19^+$ cells were SMA^+ in human LNs (MLNs, CLNs, and ALNs), and 30.3 ± 7.4% of $CCL19^+$ expressed SMA in RA ELT, where double-positive cells were closely associated to the blood vascular endothelium, whereas $CCL19^+SMA^-$ cells were mostly scattered within the aggregates.

In keeping with Page and colleagues,[11] SMA^+CCL21^+ cells in synovial ELT were found in close association to $DC\text{-}LAMP^+$ mature DCs, which are known to express CCR7,[43] suggesting a role for the ectopic stroma through the production of lymphoid chemokines in the regulation of local immune interactions (Figure 7I). Supporting this concept, despite synovial lymphatics appearing frequently devoid of cells, $DC\text{-}LAMP^+$ mature DCs were also demonstrated around and in the lumen of a proportion of $CCL21^+$ $LYVE\text{-}1^+$ vessels in the inflamed sublining (Figure 7, J and K).

Discussion

In this article, we provide evidence that, as in human SLOs, CCL21 endothelial production in chronically inflamed tissues is confined to the lymphatic apparatus and that neither flat-walled blood vessels nor HEVs of ELTs produce detectable levels of the chemokine. Our data demonstrate that the expression pattern of CCL21 within the blood vascular system is conserved across the spectrum of human lymphoid tissues, being associated with peri-ECs. This lends further support to the notion of the existence of conserved programs regulating lymphoid structural organization in homeostasis and inflammation. In keeping with this concept, we demonstrate that

Figure 7. SMA-positive can express CCL19 and co-localize with mature DCs. **A–D:** Stainings on paraffin-embedded sections of human MLN are shown. **A:** Double IHC for CCL19 (in red) and SMA (in brown) is shown on a tissue area at high magnification, demonstrating the co-localization between CCL19 and a network of spindle-shaped SMA-positive cells distributed throughout the T area. **B–D:** Color merge (**B**) and single color separations (**C** and **D**) of double IF for CCL19 (**B** and **C**; in red) and SMA (**B** and **D**; in green) confirm the co-localization between CCL19-expressing cells within the T-cell area and SMA-positive reticular cells, as revealed by yellow signal in **B**. **E–H:** Stainings on paraffin-embedded sections of rheumatoid synovial membrane are shown. **E:** Double IHC for CCL19 (in red) and SMA (in brown) reveals co-localization between CCL19 and SMA within perivascular cells in a lymphoid aggregate, indicated by **black arrows**. Some scattered CCL19-expressing cells are SMA-negative (**arrowheads**). **F–H:** Color merge (**F**) and single color separations (**G** and **H**) of double IF for CCL19 (**F** and **G**; in red) and SMA (**F** and **H**; in green) confirm the co-localization between CCL19-expressing and SMA-positive cells, as revealed by yellow signal in **F**. Note again CCL19-positive SMA-negative cells (**arrowheads**). **I–K:** Double IHC for CCL21 (in red) and the mature DC marker DC-LAMP (in brown) in rheumatoid synovium sections. **I:** In lymphoid aggregates, perivascular CCL21-expressing cells show area co-localization with DC-LAMP-positive DCs. DC-LAMP-positive DCs are also found in proximity (**J**) and within (**K**) CCL21-positive lymphatic vessels in synovial areas of cell infiltration. Original magnifications, ×1000.

extra-endothelial CCL21 is expressed by stromal cells displaying a myofibroblast-like phenotype both in human SLOs and ELTs.

The characterization of CCL21-producing vessels performed in this work relies on the use of a combination of markers specific for the lymphatic endothelium that have recently become available, such as LYVE-1,[34] podoplanin,[35] and D6.[36] CCL21$^+$ vessels in RA synovitis all expressed LYVE-1 and podoplanin, irrespectively to their localization and association with the ELT. They also were CD31$^+$[31,32] and displayed variable levels of CD34, a pan-vascular marker that is often absent from normal tissue lymphatics but can be up-regulated in certain pathological conditions, such as in tumor-associated lymphangiogenesis.[44] The combinatorial phenotype that we report here clearly indicates the lymphatic nature of CCL21$^+$ vascular structures. In keeping with this, we demonstrated that synovial CCL21$^+$ lymphatics can express variable levels of D6, a lymphatic promiscuous chemokine receptor that functions as a scavenger receptor for the internalization and neutralization of inflammatory chemokines.[36,45]

By demonstrating the lymphatic nature of CCL21-producing vessels in a subset of inflamed peripheral tissues from different diseases and of different embryological origin, we provide evidence that chronic inflammation and ectopic lymphoid neogenesis are not intrinsically associated with aberrant up-regulation of CCL21 in blood vessel and HEV endothelium. This result is in keeping with the notion that human SLO HEVs, differently from mouse, do not synthesize the chemokine[10,17] and suggests the existence of a common organizational program active in human SLOs and ELTs. Supporting this point of view, our data indicate that, inside ectopic lymphoid aggregates of inflamed peripheral tissues, the distribution of CCL21 reproduces the anatomical relationship with HEVs characterizing human SLOs,[10,17] with periendothelial localization of CCL21-producing cells and possible luminal localization of the protein through transcytosis.[17] Passive absorption or transcytosis might thus explain the decoration of some blood vessels with CCL21 that was noticed here and in previous reports when frozen sections are used[46–48] and justify the presence of naïve cells demonstrated in inflammatory sites.[5] It should be emphasized that our results do not exclude that a low rate of CCL21 transcription can be present in inflamed blood vessels, as postulated by Carlsen and colleagues[17] in SLO HEV. However, the data reported here, based on the analysis of different tissues from different diseases, demonstrate that the level of expression of CCL21 in the blood vascular compartment is similar between SLOs and ELTs and that aberrant up-regulation of CCL21 in the blood vessel endothelium is not a systematic feature of human chronic inflammation.

One of the main differences between SLOs and ELTs is the fact that, whereas SLOs also function to maintain immunosurveillance under homeostatic conditions, ELT development and function is triggered by pathological and immunological stimuli. We thus considered the possibility that, although CCL21-producing cells share a similar relationship with T cells and HEVs, the cellular sources of the chemokine could be different in terms of their stromal or hematopoietic origin in SLOs and ELTs. Our data demonstrate that CCL21 is expressed by CD45$^-$, SMA$^+$ cells both in SLOs and ELTs, indicating a common stromal origin of these cellular subsets. This pattern, which constituted the bulk of CCL21 expression in human LNs and in RA ELT, was less developed in tonsils where CCL21$^+$ SMA-negative cells were frequently observed, indicating that myofibroblast precursors or other cell types, such as DCs, may contribute to CCL21 production in specific conditions.[14,46,49] The existence of additional levels of regulation controlling SMA and CCL21 expression was also emphasized by the fact that both in normal as well as in inflamed tissues SMA$^+$ cells can be recognized in the absence of CCL21.

Our data, combined with previous observations in mice,[15] also provide evidence that, differently from ECs, the extravascular cellular sources of CCL21 are not only conserved across human lymphoid tissues but also across species. Indeed, it has been shown that in murine SLOs, the cell type responsible for CCL21 production is represented by gp38$^+$ FRCs that ensheathe the meshwork of collagen fibers (lymphoid reticular network) extending from the capsule throughout the node and encircling HEVs[15] and providing a tight regulation of chemokine and antigen delivery within SLOs.[40,50] Further studies have shown that murine FRCs also express CCL19,[15] ERTR7,[51] desmin, and SMA,[40] a reliable marker of myofibroblasts.[42] Although the specific features of this apparatus in human SLOs have been less extensively investigated,[39,52] our observations strongly indicate that CD45$^-$, CCL21$^+$, SMA$^+$ fibroblastoid cells, which we have identified in human SLOs, represent FRCs as suggested by their phenotypic marker expression, their dendroid morphology, and their reticular distribution throughout the T area and among the subcapsular sinus and HEVs. The inability to detect CCL21 expression in human SLO SMA$^+$ fibroblast cell lines in basal conditions or on *in vitro* stimulation with tumor necrosis factor-α and lymphotoxin, which have been shown to be required for normal expression of CCL21 in mouse spleen,[53] is in keeping with previous reports in murine LN FRCs.[51] This suggests that human myofibroblast-like cells may lose the capacity to express CCL21 because of *in vitro* transdifferentiation or, alternatively, that cell-contact-dependent interactions are required for the process to take place.

To our knowledge, no data at present demonstrate the possible developmental plasticity of the FRC network in human ELTs, despite experimental models of ectopic lymphoid neogenesis indicating that gp38$^+$ and ERTR7$^+$ stromal cell networks can arise ectopically, such as in the pancreas of CCL21 and CXCL13 transgenic mice.[7,54] The recognition that the stromal scaffold of the ELT in RA can acquire CCL21, CCL19, and SMA expression associated with the organization in an intra-aggregate meshwork connecting and encircling vascular structures indicates that a vestige of the lymphoid FRC network can be induced in human inflammation. Consistent with this, increased myofibroblast conversion has been reported in synovial fibroblasts derived from high-inflammation tis-

sues in association to high expression of T cell/B cell and antigen-presenting cell genes.[55] Further ultrastructural studies are required to understand the actual competence of SMA^+ fibroblastoid cells to organize functional networks and mediate antigen and chemokine delivery in human inflammatory ELTs.

In conclusion, our results indicate that CCL21 production in inflamed tissues is promoted by amplification of physiological mechanisms and ectopic reprogramming of SLO constitutive bioactivities. Our data, combined with the recent demonstration of the co-stimulatory capacity of CCL21 in T-DC interactions,[4] also emphasize the role of the tissue stroma as a third actor in the constitution of the immunological synapsis in human lymphoid tissue, suggesting the mechanisms of lymphatic and smooth muscle-positive myofibroblast differentiation in inflammation as a possible tool to interfere specifically with peripheral adaptive immune responses.

References

1. Gunn MD, Kyuwa S, Tam C, Kakiuchi T, Matsuzawa A, Williams LT, Nakano H: Mice lacking expression of secondary lymphoid organ chemokine have defects in lymphocyte homing and dendritic cell localization. J Exp Med 1999, 189:451–460
2. Nakano H, Gunn MD: Gene duplications at the chemokine locus on mouse chromosome 4: multiple strain-specific haplotypes and the deletion of secondary lymphoid-organ chemokine and EBI-1 ligand chemokine genes in the plt mutation. J Immunol 2001, 166:361–369
3. Ngo VN, Tang HL, Cyster JG: Epstein-Barr virus-induced molecule 1 ligand chemokine is expressed by dendritic cells in lymphoid tissues and strongly attracts naive T cells and activated B cells. J Exp Med 1998, 188:181–191
4. Friedman RS, Jacobelli J, Krummel MF: Surface-bound chemokines capture and prime T cells for synapse formation. Nat Immunol 2006, 7:1101–1108
5. Weninger W, Carlsen HS, Goodarzi M, Moazed F, Crowley MA, Baekkevold ES, Cavanagh LL, von Andrian UH: Naive T cell recruitment to nonlymphoid tissues: a role for endothelium-expressed CC chemokine ligand 21 in autoimmune disease and lymphoid neogenesis. J Immunol 2003, 170:4638–4648
6. Fan L, Reilly CR, Luo Y, Dorf ME, Lo D: Cutting edge: ectopic expression of the chemokine TCA4/SLC is sufficient to trigger lymphoid neogenesis. J Immunol 2000, 164:3955–3959
7. Luther SA, Bidgol A, Hargreaves DC, Schmidt A, Xu Y, Paniyadi J, Matloubian M, Cyster JG: Differing activities of homeostatic chemokines CCL19, CCL21, and CXCL12 in lymphocyte and dendritic cell recruitment and lymphoid neogenesis. J Immunol 2002, 169:424–433
8. Martin AP, Coronel EC, Sano G, Chen SC, Vassileva G, Canasto-Chibuque C, Sedgwick JD, Frenette PS, Lipp M, Furtado GC, Lira SA: A novel model for lymphocytic infiltration of the thyroid gland generated by transgenic expression of the CC chemokine CCL21. J Immunol 2004, 173:4791–4798
9. Aloisi F, Pujol-Borrell R: Lymphoid neogenesis in chronic inflammatory diseases. Nat Rev Immunol 2006, 6:205–217
10. Manzo A, Paoletti S, Carulli M, Blades MC, Barone F, Yanni G, FitzGerald O, Bresnihan B, Caporali R, Montecucco C, Uguccioni M, Pitzalis C: Systematic microanatomical analysis of CXCL13 and CCL21 in situ production and progressive lymphoid organization in rheumatoid synovitis. Eur J Immunol 2005, 35:1347–1359
11. Page G, Lebecque S, Miossec P: Anatomic localization of immature and mature dendritic cells in an ectopic lymphoid organ: correlation with selective chemokine expression in rheumatoid synovium. J Immunol 2002, 168:5333–5341
12. Barone F, Bombardieri M, Manzo A, Blades MC, Morgan PR, Challacombe SJ, Valesini G, Pitzalis C: Association of CXCL13 and CCL21 expression with the progressive organization of lymphoid-like structures in Sjogren's syndrome. Arthritis Rheum 2005, 52:1773–1784
13. Middel P, Raddatz D, Gunawan B, Haller F, Radzun HJ: Increased number of mature dendritic cells in Crohn's disease: evidence for a chemokine-mediated retention mechanism. Gut 2006, 55:220–227
14. Bonacchi A, Petrai I, Defranco RMS, Lazzeri E, Annunziato F, Efsen E, Cosmi L, Romagnani P, Milani S, Failli P, Batignani G, Lotta F, Laffi G, Pinzani M, Gentilini P, Marra F: The chemokine CCL21 modulates lymphocyte recruitment and fibrosis in chronic hepatitis C. Gastroenterology 2003, 125:1060–1076
15. Luther SA, Tang HL, Hyman PL, Farr AG, Cyster JG: Coexpression of the chemokines ELC and SLC by T zone stromal cells and deletion of the ELC gene in the plt/plt mouse. Proc Natl Acad Sci USA 2000, 97:12694–12699
16. Gunn MD, Tangemann K, Tam C, Cyster JG, Rosen SD, Williams LT: A chemokine expressed in lymphoid high endothelial venules promotes the adhesion and chemotaxis of naive T lymphocytes. Proc Natl Acad Sci USA 1998, 95:258–263
17. Carlsen HS, Haraldsen G, Brandtzaeg P, Baekkevold ES: Disparate lymphoid chemokine expression in mice and men: no evidence of CCL21 synthesis by human high endothelial venules. Blood 2005, 106:444–446
18. Baekkevold ES, Yamanaka T, Palframan RT, Carlsen HS, Rienholt FP, von Andrian UH, Brandtzaeg P, Haraldsen G: The CCR7 ligand ELC (CCL19) is transcytosed in high endothelial venules and mediates T cell recruitment. J Exp Med 2001, 193:1105–1112
19. Kriehuber E, Breiteneder-Geleff S, Groeger M, Soleiman A, Schoppmann SF, Stingl G, Kerjaschki D, Maurer D: Isolation and characterization of dermal lymphatic and blood endothelial cells reveal stable and functionally specialized cell lineages. J Exp Med 2001, 194:797–808
20. Saeki H, Moore AM, Brown MJ, Hwang ST: Cutting edge: secondary lymphoid-tissue chemokine (SLC) and CC chemokine receptor 7 (CCR7) participate in the emigration pathway of mature dendritic cells from the skin to regional lymph nodes. J Immunol 1999, 162:2472–2475
21. Debes GF, Arnold CN, Young AJ, Krautwald S, Lipp M, Hay JB, Butcher EC: Chemokine receptor CCR7 required for T lymphocyte exit from peripheral tissues. Nat Immunol 2005, 6:889–894
22. Bromley SK, Thomas SY, Luster AD: Chemokine receptor CCR7 guides T cell exit from peripheral tissues and entry into afferent lymphatics. Nat Immunol 2005, 6:895–901
23. Lira SA: A passport into the lymph node. Nat Immunol 2005, 6:866–868
24. Martin-Fontecha A, Sebastiani S, Höpken UE, Uguccioni M, Lipp M, Lanzavecchia A, Sallusto F: Regulation of dendritic cell migration to the draining lymph node: impact on T lymphocyte traffic and priming. J Exp Med 2003, 198:615–621
25. Serra HM, Eberhard Y, Martin AP, Gallino N, Gagliardi J, Baena-Cagnani CE, Lascano AR, Ortiz S, Mariani AL, Uguccioni M: Secondary lymphoid tissue chemokine (CCL21) is upregulated in allergic contact dermatitis. Int Arch Allergy Immunol 2004, 133:64–71
26. Kerjaschki D, Regele HM, Moosberger I, Nagy-Bojarski K, Watschinger B, Soleiman A, Birner P, Krieger S, Hovorka A, Silberhumer G, Laakkonen P, Petrova T, Langer B, Raab I: Lymphatic neoangiogenesis in human kidney transplants is associated with immunologically active lymphocytic infiltrates. J Am Soc Nephrol 2004, 15:603–612
27. Arnett FC, Edworthy SM, Bloch DA, McShane DJ, Fries JF, Cooper NS, Healey LA, Kaplan SR, Liang MH, Luthra HS, et al: The American Rheumatism Association 1987 revised criteria for the classification of rheumatoid arthritis. Arthritis Rheum 1988, 31:315–324
28. Hachulla E, Janin A, Flipo RM, Saile R, Facon T, Bataille D, Vanhille P, Hatron PY, Devulder B, Duquesnoy B: Labial salivary gland biopsy is a reliable test for the diagnosis of primary and secondary amyloidosis: a prospective clinical and immunohistologic study in 59 patients. Arthritis Rheum 1993, 36:691–697
29. Nagira M, Imai T, Hieshima K, Kusuda J, Ridanpaa M, Takagi S, Nishimura M, Kakizaki M, Nomiyama H, Yoshie O: Molecular cloning of a novel human CC chemokine secondary lymphoid-tissue chemokine that is a potent chemoattractant for lymphocytes and mapped to chromosome 9p13. J Biol Chem 1997, 272:19518–19524
30. Bugatti S, Caporali R, Manzo A, Vitolo B, Pitzalis C, Montecucco C: Involvement of subchondral bone marrow in rheumatoid arthritis: lymphoid neogenesis and in situ relationship to subchondral bone marrow osteoclast recruitment. Arthritis Rheum 2005, 52:3448–3459
31. Sauter B, Foedinger D, Sterniczky B, Wolff K, Rappersberger K: Immunoelectron microscopic characterization of human dermal lym-

phatic microvascular endothelial cells: differential expression of CD31, CD34, and type IV collagen with lymphatic endothelial cells vs blood capillary endothelial cells in normal human skin, lymphangioma, and hemangioma in situ. J Histochem Cytochem 1998, 46:165–176
32. Podgrabinska S, Braun P, Velasco P, Kloos B, Pepper MS, Skobe M: Molecular characterization of lymphatic endothelial cells. Proc Natl Acad Sci USA 2002, 99:16069–16074
33. Berg EL, Robinson MK, Warnock RA, Butcher EC: The human peripheral lymph node vascular addressin is a ligand for LECAM-1, the peripheral lymph node homing receptor. J Cell Biol 1991, 114:343–349
34. Banerji S, Ni J, Wang SX, Clasper S, Su J, Tammi R, Jones M, Jackson DG: LYVE-1, a new homologue of the CD44 glycoprotein, is a lymph-specific receptor for hyaluronan. J Cell Biol 1999, 144:789–801
35. Breiteneder-Geleff S, Soleiman A, Kowalski H, Horvat R, Amann G, Kriehuber E, Diem K, Weninger W, Tschachler E, Alitalo K, Kerjaschki D: Angiosarcomas express mixed endothelial phenotypes of blood and lymphatic capillaries: podoplanin as a specific marker for lymphatic endothelium. Am J Pathol 1999, 154:385–394
36. Nibbs RJB, Kriehuber E, Ponath PD, Parent D, Qin S, Campbell JDM, Henderson A, Kerjaschki D, Maurer D, Graham GJ, Rot A: The β-chemokine receptor D6 is expressed by lymphatic endothelium and a subset of vascular tumors. Am J Pathol 2001, 158:867–877
37. Bertin N, Clezardin P, Kubiak R, Frappart L: Thrombospondin-1 and -2 messenger RNA expression in normal, benign, and neoplastic human breast tissues: correlation with prognostic factors, tumor angiogenesis, and fibroblastic desmoplasia. Cancer Res 1997, 57:396–399
38. Rajkumar VS, Howell K, Csiszar K, Denton CP, Black CM, Abraham DJ: Shared expression of phenotypic markers in systemic sclerosis indicates a convergence of pericytes and fibroblasts to a myofibroblast lineage in fibrosis. Arthritis Res Ther 2005, 7:R1113–R1123
39. Thomazy VA, Vega F, Medeiros LJ, Davies PJ, Jones D: Phenotypic modulation of the stromal reticular network in normal and neoplastic lymph nodes: tissue transglutaminase reveals coordinate regulation of multiple cell types. Am J Pathol 2003, 163:165–174
40. Sixt M, Kanazawa N, Selg M, Samson T, Roos G, Reinhardt DP, Pabst R, Lutz MB, Sorokin L: The conduit system transports soluble antigens from the afferent lymph to resident dendritic cells in the T cell area of the lymph node. Immunity 2005, 22:19–29
41. Skalli O, Pelte MF, Peclet MC, Gabbiani G, Gugliotta P, Bussolati G, Ravazzola M, Orci L: Alpha-smooth muscle actin, a differentiation marker of smooth muscle cells, is present in microfilamentous bundles of pericytes. J Histochem Cytochem 1989, 37:315–321
42. Gabbiani G: The myofibroblast in wound healing and fibrocontractive diseases. J Pathol 2003, 200:500–503
43. Yanagihara S, Komura E, Nagafune J, Watarai H, Yamaguchi Y: EBI1/CCR7 is a new member of dendritic cell chemokine receptor that is up-regulated upon maturation. J Immunol 1998, 161:3096-3102
44. Fiedler U, Christian S, Koidl S, Kerjaschki D, Emmett MS, Bates DO, Christofori G, Augustin HG: The sialomucin CD34 is a marker of lymphatic endothelial cells in human tumors. Am J Pathol 2006, 168:1045–1053
45. Locati M, Martinez de la Torre Y, Galliera E, Bonecchi R, Bodduluri H, Vago G, Vecchi A, Mantovani A: Silent chemoattractant receptors: D6 as a decoy and scavenger receptor for inflammatory CC chemokines. Cytokine Growth Factor Rev 2005, 16:679–686
46. Grant AJ, Goddard S, Ahmed-Choudhury J, Reynolds G, Jackson DG, Briskin M, Wu L, Hubscher SG, Adams DH: Hepatic expression of secondary lymphoid chemokine (CCL21) promotes the development of portal-associated lymphoid tissue in chronic inflammatory liver disease. Am J Pathol 2002, 160:1445–1455
47. Armengol MP, Cardoso-Schmidt CB, Fernandez M, Ferrer X, Pujol-Borrell R, Juan M: Chemokines determine local lymphoneogenesis and a reduction of circulating $CXCR4^+$ T and CCR7 B and T lymphocytes in thyroid autoimmune diseases. J Immunol 2003, 170: 6320–6328
48. Marchal-Sommé J, Uzunhan Y, Marchand-Adam S, Valeyre D, Soumelis V, Crestani B, Soler P: Cutting edge: nonproliferating mature immune cells form a novel type of organized lymphoid structure in idiopathic pulmonary fibrosis. J Immunol 2006, 176:5735–5739
49. Lebre MC, Burwell T, Vieira PL, Lora J, Coyle AJ, Kapsenberg ML, Clausen BE, De Jong EC: Differential expression of inflammatory chemokines by Th1- and Th2-cell promoting dendritic cells: a role for different mature dendritic cell populations in attracting appropriate effector cells to peripheral sites of inflammation. Immunol Cell Biol 2005, 83:525–535
50. Gretz JE, Norbury CC, Anderson AO, Proudfoot AE, Shaw S: Lymph-borne chemokines and other low molecular weight molecules reach high endothelial venules via specialized conduits while a functional barrier limits access to the lymphocyte microenvironments in lymph node cortex. J Exp Med 2000, 192:1425–1440
51. Katakai T, Hara T, Sugai M, Gonda H, Shimizu A: Lymph node fibroblastic reticular cells construct the stromal reticulum via contact with lymphocytes. J Exp Med 2004, 200:783–795
52. Steiniger B, Barth P, Hellinger A: The perifollicular and marginal zones of the human splenic white pulp: do fibroblasts guide lymphocyte immigration? Am J Pathol 2001, 159:501–512
53. Ngo VN, Korner H, Gunn MD, Schmidt KN, Riminton DS, Cooper MD, Browning JL, Sedgwick JD, Cyster JG: Lymphotoxin alpha/beta and tumor necrosis factor are required for stromal cell expression of homing chemokines in B and T cell areas of the spleen. J Exp Med 1999, 189:403–412
54. Luther SA, Lopez T, Bai W, Hanahan D, Cyster JG: BLC expression in pancreatic islets causes B cell recruitment and lymphotoxin-dependent lymphoid neogenesis. Immunity 2000, 12:471–481
55. Kasperkovitz PV, Timmer TC, Smeets TJ, Verbeet NL, Tak PP, van Baarsen LG, Baltus B, Huizinga TW, Pieterman E, Fero M, Firestein GS, van der Pouw Kraan TC, Verweij CL: Fibroblast-like synoviocytes derived from patients with rheumatoid arthritis show the imprint of synovial tissue heterogeneity: evidence of a link between an increased myofibroblast-like phenotype and high-inflammation synovitis. Arthritis Rheum 2005, 52:430–441
56. Greenspan JS, Daniels TE, Talal N, Sylvester RA: The histopathology of Sjögren's syndrome in labial salivary gland biopsies. Oral Surg Oral Med Oral Pathol 1974, 37:217–229